

Out-of-Time-Order Correlator of Berry-Keating model

Thesis Submission

for fulfilment of the requirements for the degree of

Masters of Science

In Theoretical Physics

by

Roll: 106712

Registration: 2016-514-722



University of Dhaka

Dhaka - 1000

Abstract

Berry-Keating Hamiltonian $H_0 = \frac{1}{2}(xp + px)$ resembles the Hilbert-Pólya conjecture of Riemann Hypothesis shows quantum chaotic behavior. In this paper we first quantize xp and $1/xp$ and achieve the same spectrum with minor phase addition. We observe quantize xp and add boundary conditions to evaluate the spectrum with proper eigenfunction. Then we measured the Out-of-Time-Order Correlator (OTOC) of the Hamiltonian, to measure the quantum chaos of the Hamiltonian.

Table of Contents

1	Introduction	2
2	Semiclassical approach	8
3	Quantization of xp and $\frac{1}{xp}$	14
3.1	The Hamiltonian $H_0 = xp$	14
3.2	The inverse Hamiltonian $1/H_0$	22
4	Out-of-Time-Order Correlator of Berry-Keating	28
5	Conclusions	56

Chapter 1

Introduction

The classical zeta/ Riemann zeta function defined as $\zeta(s) = \sum_{n=1}^{\infty} \frac{1}{n^s}$ [1], where s is $s = \sigma + it$ and n is the integers. If the real part of s is greater than 1 ($\text{Re } s > 1$), the zeta function converges. But at real part equal to 1 ($\text{Re } s = 1$) it becomes the harmonic series $\zeta(1) = 1 + \frac{1}{2} + \frac{1}{3} + \frac{1}{4} + \dots$ and diverges. So there begs the question where does the zeta function go to zero. It was found that there are two types of condition that make the Riemann zeta function which is called Riemann zero or Zeta zero. For negative integers ($n = -2, -4, -6, \dots$) in the Riemann zeta function becomes zero. These types of zeros are called Trivial zeros. And the other kind of zeros, which are called Non-Trivial zeros, lie between real part of s in $\text{Re } 0 < s < 1$. Riemann hypothesized that all the non-trivial zeros lie at $s = \frac{1}{2}$. This is the famous Riemann hypothesis. Euler showed that the existing classical zeta function has a connection to the product of all prime numbers.

He proved that $\zeta(s) = \sum_{n=1}^{\infty} \frac{1}{n^s} = \prod_p \frac{1}{1-p^{-s}}$ where p is the primes. So if anyone can prove the Riemann hypothesis, they can also prove that all the prime numbers must lie on the line of $\text{Re } s = \frac{1}{2}$. It is generally agreed upon that the Riemann Hypothesis is the single most important topic in Analytic Number Theory [2, 3, 4, 5]. Hilbert-Pólya suggested that the imaginary part of the s in the Non-Trivial zeros will be a self-adjoint operator [6, 7, 8]. So the s will more look like as $s = \sigma - iE_n$. The work done by Selberg in the 1950s, in which he discovered a surprising duality between the eigenvalues of the Laplacian acting on Riemann surfaces with constant negative curvature and the length spectrum of their geodesics [9], is likely what provided the first clue of the sufficiency of this conjecture. In this work, Selberg observed that there was a relationship between the two. This link is made possible by the Selberg trace formula, which has a striking resemblance to the Riemann explicit formula. Another significant clue was provided in 1973 by the work of Montgomery, who, on the assumption that the RH was true, demonstrated that the Riemann zeros are distributed in accordance with the Gaussian Unitary Ensemble statistics of random matrix models [10]. This was a very helpful piece of information. In the 1980s, Odlyzko obtained some very spectacular numerical discoveries, which supported the conclusions that Montgomery had drawn [11]. Berry-Keating took this suggestion and proposed that the self-adjoint operator, which is E_n , will be a Hamiltonian which is $\hat{H} = \frac{1}{2}(\hat{x}\hat{p} + \hat{p}\hat{x})$. Berry-Keating also proposed that this Hamiltonian shows quantum chaotic behaviour. One can tell if any object is in chaos or chaotic

behaviour is sensitive dependence of initial condition, or we can say that a particle forget its memory about its initial condition. If a equation of a system is non-linear ODE, the system is chaotic or in chaos. Which can be describe in the following statement. Let there are two partiticle at a distance seperated by δx at time $t = 0$ or $\delta x(0)$ and after some time t the distance between the particle $\delta x(t)$, the relation of the initial and the final posotion of a chaotic system is $|\delta x(t)| \approx e^{t\lambda} |\delta x(0)|$, where t is time and λ is the Lyapunov exponent. Lyapunov exponent measures the sensitivity of initial condition.

In this paper we took the Berry-Keating Hamiltonian and also look at the Connes approach to the same Hamiltonian for evaluation of semiclassical states.[12, 13, 1] And also we look at German Sierra approach.[14]Berry and Keating used a Planck cell regularization, in which the smooth component of the Riemann zeros is represented semiclassically as discrete energy levels. Connes, on the other hand, chose an upper cutoff for the position and momenta, resulting in a semiclassical continuous spectrum devoid of smooth zeros, which all include in the paper. They both consider x and p are the 1D location and momentum of the particle. German Sierra took both of the regularization, Berry-Keating and Connes regularization and took assumption only on x or bounds x and excludes p .

Out-of-Time-Order Correlator is the measurement of chaos of quantum system. It was first introduced in a calculation of a vertex correction of a current for a superconductor[15]. The out-of-time-order correlator (OTOC) is typically defined by [16]

$$C_T \equiv -\langle [W(t), V(0)]^2 \rangle \quad (1.1)$$

where $\langle \dots \rangle$ represents the thermal average. $W(t)$ and $V(t)$ are operators as time in t in the Heisenberg representation. The OTOC, first introduced in a calculation of a vertex correction of a current for a superconductor[15], was recently turned out to be considered as a measure of the magnitude of quantum chaos. A naive argument for the relation between the OTOC and chaos is as follows[14]. Consider position and momentum operators, $x(t)$ and $p(t)$, in a quantum system. We can define an OTOC as $C_T = -\langle [x(t), p(0)]^2 \rangle$. Taking a naive semiclassical limit, we would be able to replace the commutator $[x(t), p(0)]$ by the Poisson bracket $i\hbar\{x(t), p(0)\}_{PB} = i\hbar\frac{\delta x(t)}{\delta x(0)}$. For a classically chaotic system with a Lyapunov exponent λ , we have $\frac{\delta x(t)}{\delta x(0)} \sim e^{\lambda t}$ because of sensitivity to initial condition. Thus, the OTOC should grow as $\sim \hbar^2 e^{2\lambda t}$ and we can read off the quantum Lyapunov exponent λ from it. The quantization of a classically chaotic system may provide a positive quantum Lyapunov exponent of the OTOC. Historically, the nearest neighbour distribution (NND) for the energy level spectrum has been used to quantify quantum chaos [17]. For integrable and non-integrable systems, it is considered that NNDs are given by Poisson and Wigner distributions. The OTOC is expected to be another measure of quantum chaos. A possible distinction from the classical chaotic system is that the OTOC does not grow eternally but saturates at the Ehrenfest time t_E . The Ehrenfest

time is defined by the time scale beyond which the wave function spreads over the whole system. It is roughly characterized as a boundary between a particle-like behavior and a wave-like behavior of the wave function.

In the context of AdS/CFT correspondence [18] or quantum gravity, the OTOC has gained prominence in recent years as a crucial observable. In [19], an upper bound of $2k_B T / \hbar$ was proposed for the quantum Lyapunov exponent. Black hole horizon quantum information is where the bound was first proposed [20, 21] (see also references [22, 23, 24, 25, 26]). Infinitely long range disorder interactions between Majorana fermions in the quantum mechanics of the Sachdev-Ye-Kitaev (SYK) model [27, 28] saturate the Lyapunov bound. The SYK model depicts a quantum black hole through the AdS/CFT correspondence after the quantum Lyapunov constraint is saturated.

In the definition of OTOC, we consider the thermal average of $-\langle [W(t), V(0)]^2 \rangle$. When we take thermal average, we need to consider the four point operator $\langle [W(t), V(0)]^2 \rangle$ instead of two point operator $\langle [W(t), V(0)] \rangle$. The reason is as follows. Assuming that we can replace the commutator by Poisson bracket by semiclassical limit, $\langle [W(t), V(0)] \rangle$ would also show the exponential growth $\sim e^{\lambda t}$. However, its coefficient can be both positive and negative. By taking the thermal average, their contributions would be canceled. From the quantum theory point of view, $\langle [W(t), V(0)] \rangle$ measures the correlation between $W(t)$ and $V(0)$. Therefore, the two point function decays as $t \rightarrow \infty$ and cannot show the chaotic behavior.

Now we look into the Berry-Keating and Connes semiclassical approaches

to $H = xp$

Chapter 2

Semiclassical approach

The classical Berry-Keating-Connes (BKC) Hamiltonian is[12, 29]

$$H_0^{cl} = xp \tag{2.1}$$

which has hyperbolic trajectories

$$x(t) = x_0 e^t \quad p(t) = p_0 e^{-t} \tag{2.2}$$

So the dynamics is unbounded. There is a continuous spectrum as the quantum level. Berry-Keating and Connes introduced two different types of reularizations and counted the semiclassical states. Berry-Keating introduced Plank cell in a phase space: $|x| > l_x$ and $|p| > l_p$, with $l_x l_p = 2\pi\hbar$. Connes choosed $|x| < \Lambda$ and $|p| < \Lambda$, where Λ is a cutoff. German Sierra introduced us a third regularization, $l_x < x < \Lambda$ combines the Berry-Keating

and Connes regularization position, not taking assumptions for the momenta p .

Semiclassical states number $\mathcal{N}(E)$ with an energy between 0 to E is given by

$$\begin{aligned}\mathcal{N}(E) &= \frac{A}{2\pi\hbar} \\ &= \frac{A}{h}\end{aligned}\tag{2.3}$$

Where A is the area of the allowed phase space region below the curve $E = xp$.

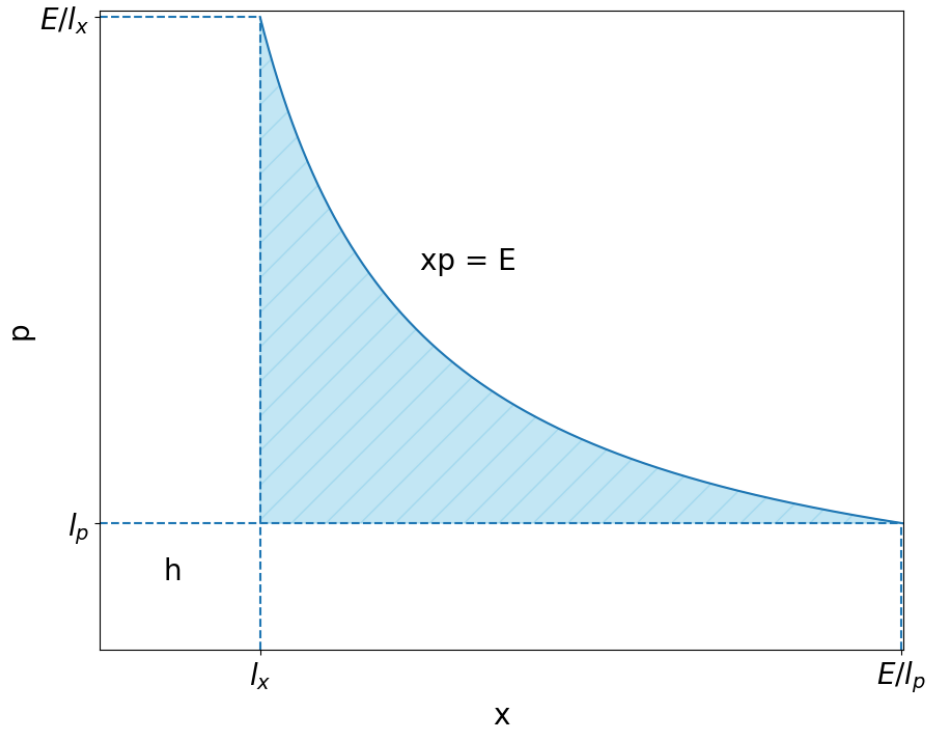


Figure 2.1: Berry-Keating Regularization

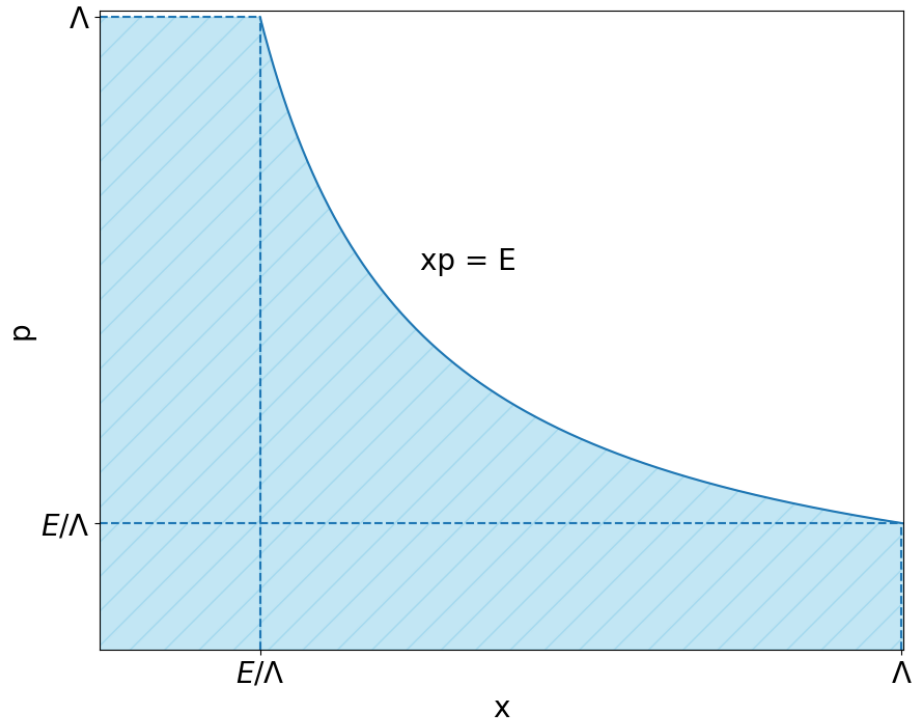


Figure 2.2: Connes Regularization
 So the the number of semiclassical states will be for Berry-Keating regu-

larization

$$\begin{aligned}
\mathcal{N}_{BK}(E) &= \frac{1}{h} \int_{l_x}^{\frac{E}{l_p}} dx \int_{l_p}^{\frac{E}{x}} dp + \\
&= \frac{1}{h} \left[\int_{l_x}^{\frac{E}{l_p}} dx \left[\frac{E}{x} - l_p \right] \right] \\
&= \frac{1}{h} \left[E \left[\ln x \right]_{l_x}^{\frac{E}{l_p}} - l_p \left[\frac{E}{l_p} - l_x \right] \right] \\
&= \frac{1}{h} \left[E \ln \frac{E}{l_x l_p} - E - l_x l_p \right] \\
&= \frac{1}{h} \left[E \ln \frac{E}{l_x l_p} - E - h \right] \\
&= \frac{E}{h} \left[\ln \frac{E}{l_x l_p} - 1 \right] + 1 \\
&= \frac{E}{2\pi\hbar} \left[\ln \frac{E}{2\pi\hbar} - 1 \right] + 1
\end{aligned} \tag{2.4}$$

adding Maslov phase $(-\frac{1}{8})$ and $\hbar = 1$, it becomes

$$\mathcal{N}_{BK}(E) = \frac{E}{2\pi} \left[\ln \frac{E}{2\pi} - 1 \right] + \frac{7}{8} +, \quad E \gg 1 \tag{2.5}$$

The exact formula for the Riemann zeros, $\mathcal{N}_R(E)$ contains a fluctuation term which depends on the zeta funcion.[1]

$$\begin{aligned}
\mathcal{N}_R(E) &= \langle \mathcal{N} \rangle + \mathcal{N}_{fl}(E) \\
\langle \mathcal{N}(E) \rangle &= \frac{1}{\pi} \text{Im} \ln \left[\Gamma \frac{1}{2} \left(\frac{1}{2} - iE \right) \right] - \frac{E}{2\pi} \ln \pi + 1 \\
\mathcal{N}_{fl}(E) &= \frac{1}{\pi} \text{Im} \ln \left[\zeta \left(\frac{1}{2} - iE \right) \right]
\end{aligned} \tag{2.6}$$

Bery-Keatin took this result and analogies between formulae in Number Theory and Quantum Chaos, they pointed the quantization of classical chaotic Hamiltonian give rise to the zeros as point like spectra.[12, 30] Whereas Connes found the number of semiclassical states diverges in the limit where the cutoff Λ goes to infinity, and that there is a finite size correction given by minus the average position of the Riemann zeros.

$$\begin{aligned}
\mathcal{N}_c(E) &= \frac{1}{h} \left[2E - \left(\frac{E}{\Lambda} \right)^2 + \int_{\frac{E}{\Lambda}}^{\Lambda} dx \int_{\frac{E}{\Lambda}}^{\frac{E}{x}} dp \right] \\
&= \frac{1}{h} \left[2E - \left(\frac{E}{\Lambda} \right)^2 + \int_{\frac{E}{\Lambda}}^{\Lambda} dx \left[\frac{E}{x} - \frac{E}{\Lambda} \right] \right] \\
&= \frac{1}{h} \left[2E - \left(\frac{E}{\Lambda} \right)^2 + E \left[\ln x \right]_{\frac{E}{\Lambda}}^{\Lambda} - \frac{E}{\Lambda} \left[\Lambda - \frac{E}{\Lambda} \right] \right] \\
&= \frac{1}{h} \left[2E - \left(\frac{E}{\Lambda} \right)^2 + E \left[\ln \frac{\Lambda^2}{E} \right] - E + \left(\frac{E}{\Lambda} \right)^2 \right] \tag{2.7} \\
&= \frac{1}{h} \left[E + E \left[\ln \frac{\Lambda^2}{E} \right] \right] \\
&= \frac{1}{h} \left[E + E \left[\ln \frac{\Lambda^2}{E} \frac{2\pi}{2\pi} \right] \right] \\
&= \frac{E}{h} \ln \frac{\Lambda^2}{2\pi} - \frac{E}{h} \left[\ln \frac{E}{2\pi} - 1 \right] \\
&= \frac{E}{2\pi} \ln \frac{\Lambda^2}{2\pi} - \frac{E}{2\pi} \left[\ln \frac{E}{2\pi} - 1 \right] \quad [taking \quad \hbar = 1]
\end{aligned}$$

This result leads to the missing spectral interpretation of the Riemann zeros, according to which there is a continuum of eigenstates (represented by the term $\frac{E}{\pi} \ln \Lambda$ in $\mathcal{N}(E)$) where states associated with Riemann zeros are

missing.

Finally, in the S-regularization the number of semiclassical states diverges as $\frac{E}{2\pi} \ln \frac{\Lambda}{l_x}$ suggesting a continuum spectrum, like in Connes's approach. But there is no finite size correction to that formula, and cosequently the possible connection to the Riemann zeros is lost.

Table 2.1:

Three different regularizations of $H = xp$ and the corresponding number of semiclassical states in units $\hbar = 1$ [\[31\]](#)

Type	Regularization	$\mathcal{N}(E)$
BK	$ x > l_x, p > l_p$	$\frac{E}{2\pi} \left(\ln \frac{E}{2\pi} - 1 \right) + 1$
C	$ x < \Lambda, p < \Lambda$	$\frac{E}{2\pi} \ln \frac{\Lambda^2}{2\pi} - \frac{E}{2\pi} \left(\ln \frac{E}{2\pi} - 1 \right)$
S	$l_x < x < \Lambda$	$\frac{E}{2\pi} \ln \frac{\Lambda}{l_x}$

Chapter 3

Quantization of xp and $\frac{1}{xp}$

3.1 The Hamiltonian $H_0 = xp$

Here we construct a self adjoint operator H_0 which acts on a Hilbert space $L^2(a, b)$ of square integrable function in the interval (a, b) . Taking $x \geq 0$, there are four possible intervals: $a = 0, l_x$ and $b = \Lambda, \infty$ where l_x and Λ were introduced (we shall take l_x and $\Lambda = N > 1$). Berry-Keating defined the quantum Hamiltonian H_0 as the normal ordered expression

$$H_0 = \frac{1}{2}(xp + px) \tag{3.1}$$

where $p = -i\hbar \frac{d}{dx}$. If $x \geq 0$, Eq. (3.1) is equivalent to

$$\begin{aligned}
H_0 &= \sqrt{x}p\sqrt{x} = -i\hbar\sqrt{x}\frac{d}{dx}\sqrt{x} \\
&= -i\hbar\left(x\frac{d}{dx} + \frac{d}{dx}x\right)
\end{aligned} \tag{3.2}$$

We know that the canonical commutation relation is

$$[\hat{x}, \hat{p}] = i\hbar \tag{3.3}$$

or, (dropping hat cause we're dealing with quantum system and operators)

$$\begin{aligned}
&[x, p] = i\hbar \\
\Rightarrow &\left[x, -i\hbar\frac{d}{dx}\right] = i\hbar \\
\Rightarrow &-i\hbar\left[x, \frac{d}{dx}\right] = i\hbar \\
\Rightarrow &\left[x, \frac{d}{dx}\right] = -1 \\
\Rightarrow &x\frac{d}{dx} - \frac{d}{dx}x = -1 \\
&\Rightarrow \frac{d}{dx}x = x\frac{d}{dx} + 1
\end{aligned} \tag{3.4}$$

Taking this value to R.H.S of Eq(3.2)

$$\begin{aligned}
-i\hbar \left(x \frac{d}{dx} + \frac{d}{dx} \right) f &= -i\hbar \left[2x \frac{d}{dx} + 1 \right] f \\
&= -i\hbar 2x \left[\frac{d}{dx} + \frac{1}{x} \frac{1}{2} \right] f \\
&= -i\hbar \frac{1}{\sqrt{x}} \frac{d}{dx} (\sqrt{x} f) \\
&= -i\hbar \frac{1}{\sqrt{x}} \frac{d}{dx} (\sqrt{x} f) \\
&= \frac{1}{\sqrt{x}} \left(-i\hbar \frac{d}{dx} \right) \sqrt{x} f
\end{aligned} \tag{3.5}$$

so

$$H_0 = \frac{1}{2} (xp + px) = -i\hbar \sqrt{x} \frac{d}{dx} \sqrt{x} \tag{3.6}$$

This is a symmetric operator acting on a certain domain of the Hilbert space $L^2(a, b)$, By definition, if an operator is symmetric (or Hermitian)[32]

$$\langle \psi | H_0 \phi \rangle = \langle \psi H_0 | \phi \rangle \tag{3.7}$$

or with limit,

$$\langle \psi | H_0 \phi \rangle - \langle \psi H_0 | \phi \rangle = i\hbar [a\psi^*(a)\phi(a) - b\phi^*(b)\psi(b)] = 0 \tag{3.8}$$

which is satisfied if both $\psi(x)$ and $\phi(x)$ vanish at the points a, b . von Neumann Theorem of deficiency indices states that, an operator is symmetric if its deficiency indices n_{\pm} are equal.[33]. Deficiency indices (or the defect numbers) of a closable symmetric operator T are cardinal number S

$$\begin{aligned}
n_+ &:= d_\lambda = \dim \mathcal{R}(T - \bar{\lambda}\mathbb{1})^\perp & \text{Im } \lambda > 0 \\
n_- &:= d_\lambda = \dim \mathcal{R}(T - \bar{\lambda}\mathbb{1})^\perp & \text{Im } \lambda < 0
\end{aligned} \tag{3.9}$$

If T is densely defined and symmetric, then T is closable, and by formula $\mathcal{N}(T^*) = \mathcal{R}(T)^\perp$

$$\begin{aligned}
n_+ &:= \dim \mathcal{N}(T^* - i\mathbb{1}) = \dim \mathcal{N}(T^* - \lambda\mathbb{1}) & \text{Im } \lambda > 0 \\
n_- &:= \dim \mathcal{N}(T^* + i\mathbb{1}) = \dim \mathcal{N}(T^* + \lambda\mathbb{1}) & \text{Im } \lambda < 0
\end{aligned} \tag{3.10}$$

By definition $n_\pm(T) = \dim \mathcal{N}(T^* \mp iT)$

Again if T is a symmetric operator, then

$$\begin{aligned}
K_+ &= \ker (i\mathbb{1} - T^*) = \text{Ran } (i\mathbb{1} - T)^\perp \\
K_- &= \ker (i\mathbb{1} + T^*) = \text{Ran } (-i\mathbb{1} + T)^\perp
\end{aligned} \tag{3.11}$$

K_+ and K_- are called the deficiency subspaces of T , The pair of numbers n_+, n_- given by $n_+(T) = \dim[K_+], n_-(T) = \dim[K_-]$ are called deficiency indices of T .

von Neumann Theorem for deficiency indices states that if T is a closed operator with deficiency indices n_+ and n_- . Then

(1) T is symmetric if and only if $n_+ = n_- = 0$ and self adjoint if $\mathcal{D}(T) = \mathcal{D}(T^*)$

(2) T is symmetric and self adjoint and also has many self adjoint extensions if and only if $n_+ = n_- \neq 0$ and $\mathcal{D}(T) = \mathcal{D}(T^*)$. There is one-one correspondence between self adjoint extensions of T and unitary maps from K_+ onto K_-

(3) If either $n_+ = 0 \neq n_-$ or $n_- = 0 \neq n_+$ then T is not symmetric and has no nontrivial self adjoint extension (such operators are called maximal symmetric operator).

So this indices counts the number of solutions of the equation, which comes from the deficiency spaces for subsystem T

$$K_{\pm} = \ker \left(-H_0^{\dagger} - \mp i\mathbb{1} \right) \quad (3.12)$$

which leads to find the solution of the equation.

$$H_0^{\dagger} \psi_{\pm} = \pm i\hbar \lambda \psi_{\pm} \quad (3.13)$$

belonging to the domain of $H_0^{\dagger}(\lambda > 0)$. If $n = n_+ = n_- > 0$, there are infinitely many self-adjoint extensions of H_0 parameterized by a unitary $n \times n$ matrix. Stone's theorem states that if $U(t)$ be a strongly continuous one parameter unitary group on a Hilbert space \mathcal{H} . Then, there is a self-adjoint operator A on \mathcal{H} so that $U(t) = e^{itA}$. The solution of the equation (3.13) is

$$\begin{aligned}
H_0^\dagger \psi_\pm &= \pm i\hbar\lambda\psi_\pm \\
\implies H_0\psi_\pm &= \pm i\hbar\lambda\psi_\pm \quad [\text{because } H_0 \text{ is self-adjoint}] \\
\implies \left(-i\hbar\sqrt{x}\frac{d}{dx}\sqrt{x}\right)\psi_\pm &= \pm i\hbar\lambda\psi_\pm \\
\implies -i\hbar\sqrt{x}\frac{d}{dx}(\sqrt{x}\psi_\pm) &= \pm i\hbar\lambda\psi_\pm \\
\implies -\sqrt{x}\frac{d}{dx}(\sqrt{x}\psi_\pm) &= \pm\lambda\psi_\pm \\
\implies -x\frac{d}{dx}\psi_\pm - \sqrt{x}\frac{1}{2\sqrt{x}}\frac{d}{dx}\psi_\pm &= \pm\lambda\psi_\pm \\
\implies -x\frac{d}{dx}\psi_\pm &= \left(\pm\lambda + \frac{1}{2}\right)\psi_\pm \\
\implies \frac{d}{dx}\psi_\pm &= -\frac{1}{x}\left(\pm\lambda + \frac{1}{2}\right)\psi_\pm \\
\implies \frac{d\psi_\pm}{\psi_\pm} &= -\frac{dx}{x}\left(\pm\lambda + \frac{1}{2}\right) \\
\implies \ln \psi_\pm &= -(\ln x)\left(\pm\lambda + \frac{1}{2}\right) + \ln C \\
\implies \psi_\pm &= Cx^{-\frac{1}{2}\mp\lambda}
\end{aligned}$$

whose norm in the interval (a,b) is

$$\begin{aligned}
\langle \psi_\pm | \psi_\pm \rangle &= \int_a^b C^2 x^{-1\mp\lambda} dx \\
&= \mp \frac{C^2}{2\lambda} (b^{\mp 2\lambda} - a^{\mp 2\lambda}) \\
&= \pm \frac{C^2}{2\lambda} (a^{\mp 2\lambda} - b^{\mp 2\lambda})
\end{aligned} \tag{3.14}$$

The deficiency indices corresponding to the four intervals considered above are collected in Table[34]. We find the deficiency indices by observing different intervals. For BK intervals $(1, \infty)$ only ψ_+ belongs to Hilbert space (ψ_- blows out. or putting intervals in Eq. (3.14) and testing whether it belongs to the Hilbert space)[31]. And the rest are given below

Table 3.1: Deficiency indices of H_0 . The corresponding intervals are associated to the semiclassical regularizations of section 2 (BK, C, S). The last one T, describes the case with no constraints on x except positivity (i.e. $x > 0$)

Type	(a,b)	(n_+, n_-)	Self-adjoint
BK	$(1, \infty)$	$(1, 0)$	-
C	$(0, N)$	$(0, 1)$	-
S	$(1, N)$	$(1, 1)$	\checkmark
T	$(0, \infty)$	$(0, 0)$	\checkmark

From the von Neumann theorem we see that H_0 is essentially self-adjoint on the half line $\mathbb{R}_+ = (0, \infty)$. This was studied by Twamley and Milbrn, who defined quantum Mellin transform using the eigenstates of H_0 [35] On the other hand, in the interval $(1, N)$ the operator H_0 admits infinitely many self-adjoint extensions parameterized by a phase $e^{i\theta}$. This phase defines the boundary condition of the functions belonging to the self-adjoint domain.[31]

$$\mathcal{D}(H_{0,\theta}) = \left\{ \psi, H_0\psi \in L^2(1, N), e^{i\theta}\psi(1) = \sqrt{N}\psi(N) \right\} \quad (3.15)$$

The eigenfunction of H_0

$$H_0\psi_E = E\psi_E, \quad (3.16)$$

are given by [12]

$$\psi_E(x) = \frac{C}{x^{\frac{1}{2}-iE\hbar}}, \quad E \in \mathbb{R} \quad (3.17)$$

where C is a normalization constant. In the half line \mathbb{R}_+ there are no further restriction on E , hence the spectrum of H_0 is continuous and covers the whole real line \mathbb{R} . In this case the normalization constant is chosen as $C = \frac{1}{\sqrt{2\pi\hbar}}$ which guarantees the standard normalization

$$\langle \psi_E | \psi_{E'} \rangle = C^2 \int_0^\infty \frac{dx}{x} x^{-i(E-E')/\hbar} = \delta(E - E') \quad (3.18)$$

In the case where H_0 is defined in the interval, the boundary condition (3.13) yields the quantization condition for E , namely

$$\begin{aligned} e^{i\theta}\psi(1) &= \sqrt{N}\psi(N) \\ \implies e^{i\theta} \frac{C}{1^{\frac{1}{2}-iE\hbar}} &= \sqrt{N} \frac{C}{N^{\frac{1}{2}-iE\hbar}} \\ \implies e^{i\theta} &= N^{-iE\hbar} \\ \implies i\theta &= \left(\frac{-iE}{\hbar}\right) \ln N \\ \implies E &= \frac{\hbar\theta}{\ln N} \\ \implies E &= \frac{2\pi\hbar}{\ln N} \left(\frac{\theta}{2\pi}\right) \end{aligned}$$

$$\implies E_n = \frac{2\pi\hbar}{ln} \left(n + \frac{\theta}{2\pi}\right) \quad n \in \mathbb{N} \quad (3.19)$$

Hence the spectrum of H_0 is discrete, with a level spacing decreasing for largerm values of N . The normalization constant of the wave function is now $C = \frac{1}{\sqrt{ln} N}$ which gives,

$$\langle \psi_{E_n} | \psi_{E_{n'}} \rangle = C^2 \int_1^N \frac{dx}{x} x^{-i(E_n - E_{n'})/\hbar} = \delta_{n,n'} \quad (3.20)$$

The spectrum (3.13) agrees with the semiclassical result given in Table 1 for the S-regularization(recall that $l_x = 1, \Lambda = N, \hbar = 1$) For the particular case where $\theta = \pi$, one observes that the energy spectrum is symmetric around zero, i.e, if E_n is an eigenenergy so is $-E_n$. This result is obtained in working[36] with the inverse Hamiltonian $\frac{1}{H_0}$. We are reviewing that construction in next section.

3.2 The inverse Hamiltonain $1/H_0$

First, we take the expression at Eq(3.8) and take the formal inverse, i.e., $H_0^{-1} = x^{1/2}p^{-1}x^{1/2}$. The operator p^{-1} is the one-dimensional Green's function with matrix elements(definition of Green's function: Green's function is the kernel of and integral operator that represents the inverse of a differential operator. Let

$$Lu = f \quad (3.21)$$

Here u and f are vectors and L is a square, invertible matrix. The inverse matrix exists if $\lambda = 0$ is not an eigenvalue of L , or when $\det L \neq 0$. Now

$$u = L^{-1}f \quad (3.22)$$

where L^{-1} is the inverse operator of L . The inverse operator to be an integral operator of the form.

$$(L^{-1}f)(x) = \int_a^b g(x, \xi) f(\xi) d\xi \quad (3.23)$$

with kernel G . If L exists, then the kernel function $g(x, \xi)$ is called the Green's function associated with L .

So p^{-1} operator will be

$$\begin{aligned} \langle x | p^{-1} | x' \rangle &= \left\langle x \left| \frac{1}{-i\hbar \frac{d}{dx}} \right| x' \right\rangle \\ &= -i\hbar \left\langle x \left| \frac{1}{\frac{d}{dx}} \right| x' \right\rangle \\ &= \frac{\hbar}{i} G(x, x') \\ &= \frac{\hbar}{2i} \text{sign}(x - x') \end{aligned} \quad (3.24)$$

Here $\text{sign}(x - x')$ is the sign function, [36]. The operator H_0^{-1} is defined in the interval $(1, N)$ by the continuous matrix,

$$H_0^{-1}(x, x') = \frac{i}{2\hbar} \frac{\text{sign}(x - x')}{\sqrt{xx'}}, \quad 1 \leq x, x' \leq N. \quad (3.25)$$

It's spectrum is found solving the Schrödinger equation.

$$\begin{aligned} H_0(x, x')\psi(x') &= E\psi(x) \\ \implies H_0^{-1}(x, x')\psi(x') &= E^{-1}\psi(x) \\ \implies \frac{i}{2\hbar} \int_1^N dx' \frac{\text{sign}(x - x')}{\sqrt{xx'}} \psi(x') &= E^{-1}\psi(x) \end{aligned} \quad (3.26)$$

for the eigenvalue E^{-1} , which must not be singular for H_0^{-1} to be invertible. Define a new wave function

$$\phi(x) = \frac{\psi(x)}{\sqrt{x}} \quad (3.27)$$

which satisfies

$$\frac{iE}{2\hbar} \int_1^N dx' \text{sign}(x - x') \phi(x') = x\phi(x) \quad (3.28)$$

Taking derivative with respect to x

$$\begin{aligned}
\frac{d}{dx} \left(\frac{iE}{2\hbar} \int_1^N dx' \text{sign}(x - x') \phi(x') \right) &= \frac{d}{dx} (x\phi(x)) \\
\Rightarrow \frac{iE}{2\hbar} \int_1^N dx' 2\delta(x - x') \phi(x') &= \phi(x) + x \frac{d}{dx} \phi(x) \\
\Rightarrow \frac{iE}{\hbar} \phi(x) &= \phi(x) + x \frac{d}{dx} \phi(x) \\
\Rightarrow x \frac{d}{dx} \phi(x) &= \left(1 - \frac{iE}{\hbar} \right) \phi(x) \\
\Rightarrow \frac{d\phi(x)}{\phi(x)} &= \left(1 - \frac{iE}{\hbar} \right) \frac{dx}{x} \\
\Rightarrow \ln \phi(x) &= \left(1 - \frac{iE}{\hbar} \right) \ln x + \ln C \\
\Rightarrow \phi(x) &= \frac{C}{x^{1 - \frac{iE}{\hbar}}}
\end{aligned} \tag{3.29}$$

$$\psi(x) = \frac{C}{x^{1/2 - \frac{iE}{\hbar}}} \tag{3.30}$$

with $C = \frac{1}{\sqrt{\ln N}}$ as in Eq(3.22). Eq(3.27) fixes the functional form of $\psi(x)$.

To find the spectrum we impose (3.30) at one point, say $x = 1$, obtaining,

$$\begin{aligned}
\frac{iE}{2\hbar} \int_1^N dx' \text{sign}(1 - x') \phi(x') &= \phi(1) \\
\Rightarrow \frac{iE}{2\hbar} \int_1^N dx' \text{sign}(1 - x') \frac{C}{x'^{1 - iE/\hbar}} &= \frac{C}{1^{1 - iE/\hbar}} \\
\Rightarrow \frac{iE}{2\hbar} \int_1^N dx' \text{sign}(1 - x') \frac{1}{x'^{1 - iE/\hbar}} &= 1
\end{aligned} \tag{3.31}$$

we know that sign function

$$\text{sign}(1 - x') = \begin{cases} 1 & 1 - x' > 0 \implies 1 > x' \\ 0 & 1 - x' = 0 \implies 1 = x' \\ -1 & 1 - x' < 0 \implies 1 < x' \end{cases}$$

Therefore

$$\frac{-iE}{2\hbar} \int_1^N dx' x'^{-1+iE/\hbar} = 1$$

$$\frac{-iE}{2\hbar} \left[\frac{x'^{iE/\hbar}}{iE/\hbar} \right]_1^N = 1$$

$$\frac{1}{2} [N^{iE/\hbar} - 1^{iE/\hbar}] = 1$$

$$N^{iE/\hbar} - 1 = -2$$

$$N^{iE/\hbar} = -1$$

$$N^{iE/\hbar} = e^{i\pi}$$

$$\frac{iE}{\hbar} \ln N = i\pi$$

$$E = \frac{\pi\hbar}{\ln N}$$

$$E = \frac{2\pi\hbar}{\ln N} \frac{1}{2}$$

$$\therefore E_n = \frac{2\pi\hbar}{\ln N} \left[n + \frac{1}{2} \right] \quad (3.32)$$

This sprectrum coincides with (3.19) for $\theta = \pi$, so that the eigenstates come in pairs $\{E_n, -E_n\}$ as corresponds to an Hermitian antisymmetric operator. Including a BCS coupling , related to θ yields the spectrum (3.19)[35]

We take this spectrum and wavefunction to calculate OTOC(out of time order correlator)

Chapter 4

Out-of-Time-Order Correlator of Berry-Keating

First we formulate how to calculate the OTOC for generic quantum mechanics. In particular, by the reason described above, we choose $W = x$ and $V = p$ to measure a possible indication of quantum chaos. We consider the out-of-time-order correlator (OTOC) defined by

$$C_T \equiv -\langle [x(t), p(0)]^2 \rangle \quad (4.1)$$

where $\langle \mathcal{O} \rangle \equiv \frac{\text{tr}[e^{-\beta H} \mathcal{O}]}{\text{tr} e^{-\beta H}}$. Here we define $\frac{1}{\beta}$ with the temperature of the system T . We will omit the argument of Heisenberg operators for $t = 0$; $\mathcal{O} \equiv \mathcal{O}(0)$. Taking energy eigenstates as the basis of the Hilbert space, we can rewrite the OTOC as

$$C_T(t) = \frac{1}{Z} \sum_n e^{-\beta E_n} c_n(t) \quad (4.2)$$

$$c_n \equiv - \langle n | [x(t), p(0)]^2 | n \rangle \quad (4.3)$$

where $H |n\rangle = E_n |n\rangle$. We will refer the OTOC for a fixed energy eigenstate, $c_n(t)$, as a microcanonical OTOC. On the other hand, we will refer $C_T(t)$ as a thermal OTOC. Once we compute microcanonical OTOCs, we can obtain the thermal OTOC by taking their thermal average. Let us rewrite the microcanonical OTOC using matrix element of x and p for numerical calculations. Using the completeness relation $1 = \sum_m |m\rangle \langle m|$, we rewrite the microcanonical OTOC as

$$c_n(t) = \sum_m b_{nm}(t) b_{nm}^*(t) \quad (4.4)$$

$$b_{nm}(t) \equiv -i \langle n | [x(t), p(0)] | m \rangle \quad (4.5)$$

Note that $b_{nm}(t)$ is Hermitian: $b_{nm}(t) = b_{nm}^*(t)$. Substituting $x(t) = e^{iHt} x e^{-iHt}$ and inserting the completeness relation again, we obtain

$$\begin{aligned}
b_{nm}(t) &= -i \langle n | [e^{iHt} x e^{-iHt}, p] | m \rangle \\
&= -i \langle n | [e^{iHt} x e^{-iHt} p - p e^{iHt} x e^{-iHt}] | m \rangle \\
&= -i \left[\sum_k \langle n | e^{iHt} x e^{-iHt} | k \rangle \langle k | p | m \rangle - \sum_k \langle n | p | k \rangle \langle k | e^{iHt} x e^{-iHt} | m \rangle \right] \\
&= -i \left[\sum_k \langle n | e^{iE_n t} x e^{-iE_k t} | k \rangle \langle k | p | m \rangle - \sum_k \langle n | p | k \rangle \langle k | e^{iE_k t} x e^{-iE_m t} | m \rangle \right] \\
&= -i \sum_k [e^{iE_{nk} t} x_{nk} p_{km} - e^{iE_{km} t} p_{nk} x_{km}]
\end{aligned}$$

$$\therefore b_{nm}(t) = -i \sum_k [e^{iE_{nk} t} x_{nk} p_{km} - e^{iE_{km} t} p_{nk} x_{km}] \quad (4.6)$$

where $E = E_n - E_m$, $x_{nm} \equiv \langle n | x | m \rangle$, $p_{nm} \equiv \langle n | p | m \rangle$. In this expression, there are matrix components of p . They are not desirable since numerical derivatives of wave functions lose the numerical accuracy. For a natural Hamiltonian with the form,

$$H = \sum_{i=1}^N p_i^2 + U(x_1, \dots, x_N) \quad (4.7)$$

we can express p_{nm} using x_{nm} . We know from canonical commutation relation

$$[x, p] = i \quad (\hbar = 1)$$

Therefore

$$\begin{aligned} [H, x] &= [p^2 + U(x), x] \\ &= [p^2, x] + [U(x), x] \\ &= p[p, x] + [p, x]p \\ &= -ip - ip \end{aligned}$$

$$\therefore [H, x] = -2ip \quad (4.8)$$

Applying $\langle m | \cdots | n \rangle$ to the both sides of the equation, we obtain

$$\begin{aligned} \langle m | [H, x] | n \rangle &= \langle m | -2ip | n \rangle \\ \langle m | (Hx - xH) | n \rangle &= -2i \langle m | p | n \rangle \\ \langle m | (E_m x - x E_n) | n \rangle &= -2ip_{mn} \\ E_{mn} x_{mn} &= -2ip_{mn} \\ p_{mn} &= \frac{i}{2} E_{mn} x_{mn} \end{aligned}$$

Substituting this expression into (4.6) we have

$$b_{nm}(t) = \frac{-i\hbar}{2} \sum_k (e^{iE_{nk}t} x_{nk} E_{km} x_{km} - e^{iE_{km}t} E_{nk} x_{nk} x_{km})$$

$$b_{nm}(t) = \frac{1}{2} \sum_k x_{nk} x_{km} (E_{km} e^{iE_{nk}t} - E_{nk} e^{iE_{km}t}) \quad (4.9)$$

Now we can take this equation to calculate OTOC of Berry-Keating Hamiltonian from (3.32). The spectrum is

$$E_n = \frac{2\pi\hbar}{\ln N} \left[n + \frac{1}{2} \right] \quad (4.10)$$

and the wavefunction

$$\psi(x) = \frac{C}{x^{1/2 - \frac{iE}{\hbar}}} \quad (4.11)$$

from here we can evaluate $x_{nm} = \langle n | x | m \rangle$ value

$$\begin{aligned}
\langle \psi_E | x | \psi_{E'} \rangle &= C^2 \int_1^N \frac{dx}{x} x^{-i(E-E')/\hbar} x \\
&= C^2 \int_1^N dx x^{-i(E-E')/\hbar} \\
&= C^2 \left[\frac{x^{1-i(E-E')/\hbar}}{1-i(E-E')/\hbar} \right]_1^N \\
&= C^2 \frac{1}{1-i(E-E')/\hbar} \left[N^{1-i(E-E')/\hbar} - 1 \right] \\
&= C^2 \frac{1}{1-i(E-E')/\hbar} \left[N^{1-i(E-E')/\hbar} - 1 \right]
\end{aligned}$$

Therefore, $\langle n | x | m \rangle = x_{nm}$ is

$$\langle n | x | m \rangle = \frac{1}{\ln N} \frac{1}{1 - i \frac{2\pi\hbar}{\ln N} (n + \frac{1}{2} - m - \frac{1}{2})/\hbar} \left[N^{1-i \frac{2\pi\hbar}{\ln N} (n + \frac{1}{2} - m - \frac{1}{2})/\hbar} - 1 \right] \quad (4.12)$$

$$x_{nm} = \frac{1}{\ln N} \frac{1}{1 - i \frac{2\pi}{\ln N} (n + \frac{1}{2} - m - \frac{1}{2})} \left[N^{1-i \frac{2\pi}{\ln N} (n + \frac{1}{2} - m - \frac{1}{2})} - 1 \right] \quad (4.13)$$

putting these values on Eq(4.9)

$$b_{nm}(t) = \frac{1}{2} \sum_k x_{nk} x_{km} (E_{km} e^{iE_{nk}t} - E_{nk} e^{iE_{km}t})$$

and calculate OTOC analytically. cause carry out the summation of x_{nm} and energy eigenstates makes things little complicated. The graph and codes are given below.

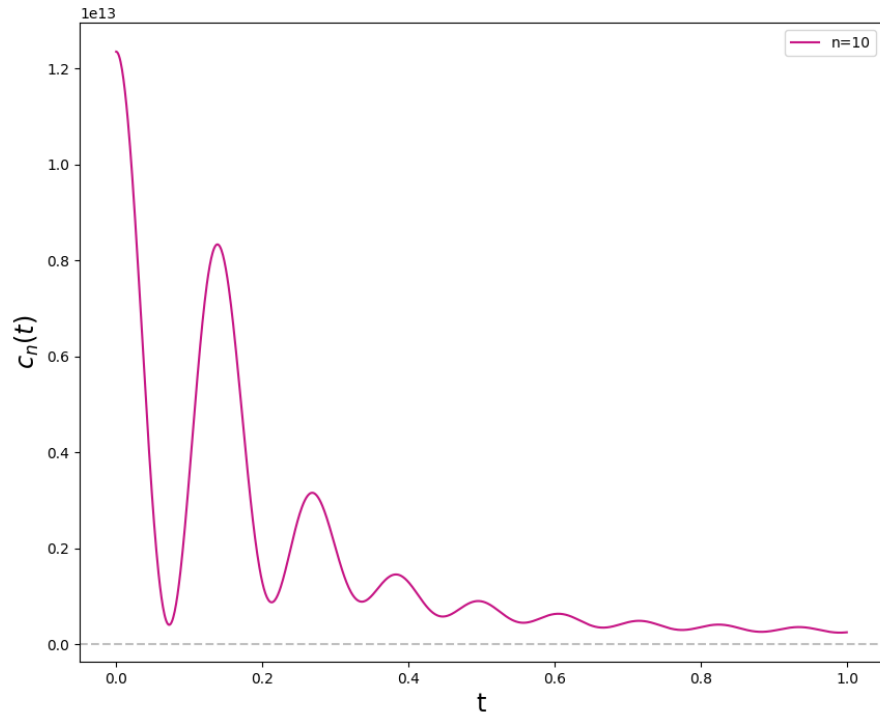


Figure 4.1

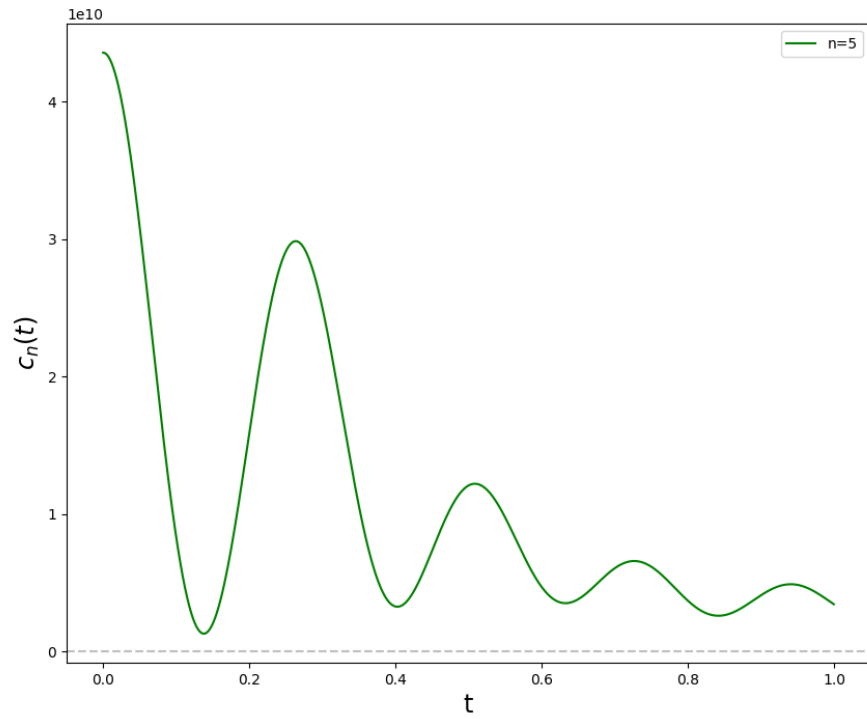


Figure 4.2

Here microcanonical OTOC and thermal OTOC are same with different temperatures.

```

1 import numpy as np
2 import matplotlib.pyplot as plt
3 import math
4 import cmath
5
6 a = [] #initialize some list to plot data
7 b = []
8 r=6    # matrix dimension number

```

```

9 N=10      #Higest interval in the spectrum
10 T=40      #temperature
11
12
13 #function for spetrum E_{nm}
14 def E(n, m):
15     return (2*math.pi*(n-m))/(math.log(N))
16
17
18 #function for position x_{nm}
19 def x(n, m):
20     a = (1/1-(2j*math.pi*(n-m)/math.log(N)))/(math.sqrt(math.
21     log(N)))
22     b = (N**(1-(2j*math.pi*(n-m)/math.log(N)))-1)
23     return a*b
24
25 #calculating Thermal OTOC C_{T}
26 for t in np.arange(0,1,0.001):
27     Z=0
28     C=0
29     s3=0
30
31     for n in range(0,r):
32         s2 = 0
33
34         for m in range(0,r):

```

```

35         s1=0
36
37         for k in range(0,r):
38             s1 += (1/2.0)*x(n,k)*x(k,m)*(E(k,m)*cmath.exp
(1j*E(n,k)*t) - E(n,k)*cmath.exp(1j*E(k,m)*t))
39
40             s2 += s1*np.conjugate(s1)
41
42         #partition function
43         Z += cmath.exp(-E(n,0)/T)
44
45         #e^{-\beta E_n} 0
46         C += (cmath.exp(-E(n,0)/T)*s2)
47
48         #expectation value or Thermal OTOC
49         s3=C/Z
50
51
52         a.append(t)
53         b.append(s3)
54
55
56 #for plot
57 f = plt.figure()
58 f.set_figwidth(10)
59 f.set_figheight(8)
60 plt.plot(a, b, label='n=10', color='mediumvioletred')

```

```

61 plt.ylabel('$c_{n}(t)$', fontsize=30)
62 plt.xlabel('t', fontsize=30)
63 plt.legend()
64 plt.show()
65
66
67
68 f = plt.figure()
69 f.set_figwidth(10)
70 f.set_figheight(8)
71 plt.plot(a, b, label='n=5', color='green')
72 plt.ylabel('$c_{n}(t)$', fontsize=30)
73 plt.xlabel('t', fontsize=40)
74 plt.axhline(0, ls='--', alpha=0.5, c='grey')
75 plt.legend()
76 plt.savefig('test.png')

```

Listing 4.1: Python example

We also used Markov Chain Monte Carlo Method/Hamiltonian Monte Carlo Method [37, 38] and obtained same result. The graph and codes are given below.

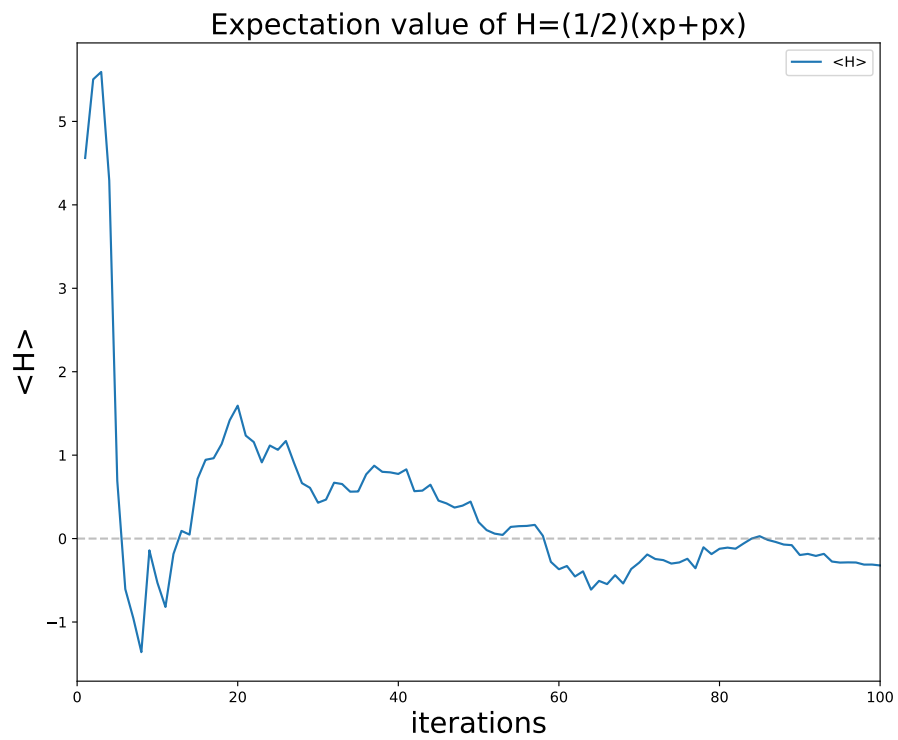


Figure 4.3

```

1 #ifndef MATRIX
2 #define MATRIX
3
4
5 #include <complex>
6 using namespace std;
7
8 //matrix dimension
9 const int n=10;
10

```

```

11
12 /*
13     Declaring a function for easily calling a matrix, it 2nd,
14     3rd, 4th order terms, and their traces.
15 */
16 double matrix(complex<double> A[n][n], complex<double> (&A2)[
17     n][n], complex<double> (&A3)[n][n], complex<double> (&A4)[
18     n][n], double& s, double& s2, double& s3, double& s4)
19 {
20     s=0, s2=0, s3=0, s4=0;
21
22     // 2nd Order matrix
23     for(int i=0; i<n; i+=1)
24     {
25         for(int j=0; j<n; j+=1)
26         {
27             for(int k=0; k<n; k+=1)
28             {
29                 A2[i][j] += A[i][k]*A[k][j];
30             }
31         }
32     }
33
34     // 3rd order matrix
35     for(int i=0; i<n; i+=1)
36     {
37         for(int j=0; j<n; j+=1)

```

```

35     {
36         for(int k=0; k<n; k+=1)
37         {
38             A3[i][j] += A2[i][k]*A[k][j];
39         }
40     }
41 }
42
43 // 4th order matrix
44 for(int i=0; i<n; i+=1)
45 {
46     for(int j=0; j<n; j+=1)
47     {
48         for(int k=0; k<n; k+=1)
49         {
50             A4[i][j] += A3[i][k]*A[k][j];
51         }
52     }
53 }
54
55 // Trace of A
56 for(int i=0; i<n; i+=1)
57 {
58     s += A[i][i].real();
59 }
60
61 // Trace of A^2

```

```

62     for(int i=0; i<n; i+=1)
63     {
64         s2 += A2[i][i].real();
65     }
66
67     // Trace of A^3
68     for(int i=0; i<n; i+=1)
69     {
70         s3 += A3[i][i].real();
71     }
72
73     // Trace of A^4
74     for(int i=0; i<n; i+=1)
75     {
76         s4 += A4[i][i].real();
77     }
78
79     return 0;
80 }
81
82 #endif

```

Listing 4.2: matrix.h

```

1  #ifndef BOX
2  #define BOX
3
4

```

```

5 #include<cstdlib>
6 #include<cmath>
7 #include<random>
8 using namespace std;
9
10
11 //Gaussian Random Number Generator with Box Muller Algorithm
12 double Box(double& x, double& y)
13 {
14     //uniform random numbers between 0 and 1
15     random_device rd;
16     mt19937 mt(rd());
17     uniform_real_distribution<double> r1(0, 1);
18     double p,q;
19
20     p = r1(mt);
21     q = r1(mt);
22
23
24     //Gaussina random numbers with weights proportional to e
    ^{-x^2/2} and e^{-y^2/2}
25     x = sqrt(-2*log(p))*sin(2*M_PI*q);
26     y = sqrt(-2*log(p))*cos(2*M_PI*q);
27
28
29     return 0;
30 }

```

```

31
32 #endif

```

Listing 4.3: box.h

```

1  #ifndef HAM
2  #define HAM
3
4
5
6  /*
7      Calculating Hamiltonian of Berry-Keating  $H = (1/2)(xp+px)$ 
8  */
9  double hamiltonian(complex<double> A[n][n], complex<double> B
10     [n][n])
11 {
12     // A is a matrix of x
13     // B is a matrix of p
14     complex <double> H[n][n] = {0}, N1[n][n] = {0}, N2[n][n]
15     = {0};
16     double sum=0;
17
18     for(int i=0; i<n; i+=1)
19     {
20         for(int j=0; j<n; j+=1)
21         {

```

```
22         for(int k=0; k<n; k+=1)
23         {
24             // x*p
25             N1[i][j] += A[i][k]*B[k][j];
26         }
27     }
28 }
29
30
31 for(int i=0; i<n; i+=1)
32 {
33     for(int j=0; j<n; j+=1)
34     {
35         for(int k=0; k<n; k+=1)
36         {
37             // p*x
38             N2[i][j] += B[i][k]*A[k][j];
39         }
40     }
41 }
42
43
44 for(int i=0; i<n; i+=1)
45 {
46     for(int j=0; j<n; j+=1)
47     {
48         // xp + px
```

```

49         H[i][j] = N1[i][j] + N2[i][j];
50     }
51 }
52
53
54 for(int i=0; i<n; i+=1)
55 {
56     sum += H[i][i].real();
57 }
58
59
60 return 0.5*sum;
61 }
62
63
64 #endif

```

Listing 4.4: hamiltonian.h

```

1 #ifndef FORCE
2 #define FORCE
3
4 #include <~/matrix.h>
5
6
7 /*
8     Calculating force (dH/d phi = dS/d phi) term = p
9 */

```



```

10
11 double force(complex<double> A[n][n], complex<double> (&dh)[n
    ][n])
12 {
13     // calculating force matrix
14     for(int i=0; i<n; i+=1)
15     {
16         for(int j=0; j<n; j+=1)
17         {
18             // dh = dH/dphi
19             dh[i][j] = (A[i][j]);
20         }
21     }
22
23     return 0;
24 }
25
26 #endif

```

Listing 4.5: force.h

```

1 #ifndef MOL
2 #define MOL
3
4 #include<~/box.h>
5 #include<~/force.h>
6 #include<~/hamiltonian.h>
7

```

```

8
9
10 /*
11     Molecular dynamics part
12 */
13 double molecular(complex<double> (&phi)[n][n], complex<double>
14     > (&P)[n][n], double& hi, double& hf)
15 {
16     double p, q, r1, r2, nt=10;
17
18     complex<double> dt=0.001, dh[n][n] = {0};
19
20     for(int i=0; i<n; i+=1)
21     {
22         for(int j=0; j<n; j+=1)
23         {
24             Box(p,q);
25             P[i][j] = complex(p/sqrt(2),q/sqrt(2));
26         }
27     }
28
29     // Initial hamiltonian of molecular dynamics
30     hi = hamiltonian(phi,P);
31
32
33     //leap frog method

```

```

34 // xi(dt/2) = xi(0) + pi(0)dt/2;
35 for(int i=0; i<n; i+=1)
36 {
37     for(int j=0; j<n; j+=1)
38     {
39         phi[i][j] += 0.5*P[i][j]*dt;
40     }
41 }
42
43 // for n=1 to nt steps
44 //pi(ndt) = pi((n-1)dt) - (ds/dx)((n-1/2)dt)dt
45 for(int i=1; i<=nt-1; i+=1)
46 {
47     //calling force term
48     force(P,dh);
49     for(int j=0; j<n; j+=1)
50     {
51         for(int k=0; k<n; k+=1)
52         {
53             P[j][k] -= dh[j][k]*dt;
54             phi[j][k] += P[j][k]*dt;
55         }
56     }
57 }
58
59 //calling force term
60 //late step of leap frog method

```

```

61 //pi(nt *dt) = pi((nt-1)dt) - (ds/dx)((nt-1/2)dt)dt
62 //xi(nt* dt) = xi((nt-1)dt) + p(nt *dt) dt/2;
63 force(P,dh);
64 for(int i=0; i<n; i+=1)
65 {
66     for(int j=0; j<n; j+=1)
67     {
68         P[i][j] -= dh[i][j]*dt;
69         phi[i][j] += 0.5*P[i][j]*dt;
70     }
71 }
72
73 //final hamiltonian of molecular dynamics
74 hf = hamiltonian(phi,P);
75
76 return 0;
77 }
78
79 #endif

```

Listing 4.6: molecular.h

```

1 #include <~/box.h>
2 #include <~/force.h>
3 #include <~/molecular.h>
4 #include <~/matrix.h>
5 #include <iostream>
6 #include <cmath>

```

```

7  #include <fstream>
8  #include <cstdlib>
9  #include <complex>
10 #include <ctime>
11 #include <random>
12 using namespace std;
13
14 double fact(double x)
15 {
16     double s=1;
17     for(int i=1; i<=x; i+=1)
18     {
19         s *= i*(i+1);
20     }
21
22     return s;
23 }
24
25 int main()
26 {
27     srand(time(NULL));
28     ofstream fout("main.dat");
29     ofstream file("part.dat");
30     double hi, hf, s=0, s2=0, r,
31     c=0,p,q,C[10000]={},x=0,a=0, D[10000][10]={};
32     long double x1=0, x2, y1=0, y2=0;
33     const int n=10;

```

```

34     double t = 198;
35     //x=0;
36     complex<double> A[n][n] = {0},
37     A0[n][n] = {0}, B[n][n] = {0}, B0[n][n] = {0};
38
39     //generating random value for x
40     for(int i=0; i<n; i+=1)
41     {
42         for(int j=0; j<n; j+=1)
43         {
44             p=(double)rand()/((double)RAND_MAX);
45             q=(double)rand()/((double)RAND_MAX);
46             A[i][j]=complex(p,q);
47         }
48     }
49
50     //metropolis test
51     for(int i=1; i<10000; i+=1)
52     {
53         for(int j=0; j<n; j+=1)
54         {
55             for(int k=0; k<n; k+=1)
56             {
57                 //x0=x
58                 A0[j][k] = A[j][k];
59             }
60         }

```

```

61         }
62
63         molecular(A,B,hi,hf);
64         r = (double)rand()/(double)RAND_MAX;
65         if(exp(hi-hf)>r)
66         {
67             c+=1;
68         }
69
70         else
71         {
72             for(int j=0; j<n; j+=1)
73             {
74                 for(int k=0; k<n; k+=1)
75                 {
76                     A[j][k] = A0[j][k];
77                 }
78             }
79         }
80
81         s = hamiltonian(A,B);
82         s2 += hamiltonian(A,B);
83         C[i] = s;
84         fout << i << " " << (double)s/(double)i
85         << " " << (double)s2/(double)(i) << endl;
86     }
87

```

```

88     //calculating partition function
89     y1=0, x1=0;
90     for(int i=1; i<10000; i+=1)
91     {
92         y1 += exp(-C[i]/t);
93
94     }
95
96     // sum of <H>*exp(-\beta H)/Z
97     for(int i=1; i<10000; i+=1)
98     {
99         x1 += C[i]*exp(-C[i]/t);
100
101         file << i << " " << x1/y1 << endl;
102
103     }
104
105
106
107     return 0;
108 }

```

Listing 4.7: main.cpp

```

1 import numpy as np
2 import matplotlib.pyplot as plt
3
4 a = np.loadtxt("main.dat")

```



```

5
6 f = plt.figure()
7 f.set_figwidth(10)
8 f.set_figheight(8)
9 plt.plot(a[:,0], a[:,2], label='<H>')
10 plt.xlim([0,100])
11 plt.axhline(0, c='grey', alpha=0.5, ls='--')
12 plt.xlabel("iterations", fontsize=20)
13 plt.ylabel("<H>", fontsize=20)
14 plt.title("Expectation value of  $H=(1/2)(x_p+p_x)$ ", fontsize=20)
15 plt.legend()
16 plt.show()
17
18
19 f = plt.figure()
20 f.set_figwidth(10)
21 f.set_figheight(8)
22 plt.plot(a[:,0], a[:,2], label='<H>')
23 plt.xlim([0,100])
24 plt.axhline(0, c='grey', alpha=0.5, ls='--')
25 plt.xlabel("iterations", fontsize=20)
26 plt.ylabel("<H>", fontsize=20)
27 plt.title("Expectation value of  $H=(1/2)(x_p+p_x)$ ", fontsize=20)
28 plt.legend()
29 plt.savefig("plot.pdf")

```

Listing 4.8: plot.py

Chapter 5

Conclusions

In this paper, we discussed what is Riemann hypothesis is, and why it is important to the field to quantum mechanics. The imaginary part of Hamiltonian proposed by Berry-Keating Hamiltonian $H_0 = \frac{1}{2}(xp + px)$ shows the self-adjoint and quantum chaos. We look at Sierra regularization of Berry-Keating Hamiltonian, and their intervals $l_x = 1, \Lambda = 1$ and evaluated the spectrum $E_n = \frac{2\pi\hbar}{\ln N}(n + \frac{\theta}{2\pi})$ of $\psi_E(x) = \frac{C}{x^{\frac{1}{2}-iE\hbar}}$ eigenfunction. Then we look at the quantization of inverse Hamiltonian $H_0^{-1} = x^{-1/2}p^{-1}x^{1/2}$ and obtained the spectrum $E_n = \frac{2\pi\hbar}{\ln N}(n + \frac{1}{2})$ which is reckon to be $E_n = \frac{2\pi\hbar}{\ln N}(n + \frac{\theta}{2\pi})$ with $\theta = \pi$

We discussed OTOC in quantum mechanics and its thermal and microcanonical relation between them. We input the spectrum and position operator of inverse Hamiltonian and calculate its quantum chaos analytically. We see that microcanonical OTOC settles at value greater than zero while

the thermal OTOC displays the same behaviour of microcanonical OTOC.

Bibliography

- [1] Edwards HM Riemanns Zeta Function. Academic press new york, 1974.
- [2] Edwards HM Riemanns Zeta Function. Academic press new york, 1974.
- [3] Edward Charles Titchmarsh, David Rodney Heath-Brown, Edward Charles Titchmarsh Titchmarsh, et al. *The theory of the Riemann zeta-function*. Oxford university press, 1986.
- [4] Enrico Bombieri. Problems of the millennium: The riemann hypothesis. *Clay Mathematics Institute*, 2000.
- [5] Peter Sarnak. Problems of the millennium: The riemann hypothesis (2004). *Pàgina web de la fundació Clay*, 2004.
- [6] See m. watkins, <http://secamlocal.ex.ac.uk/~mwatkins/zeta/-physics.html>, for a comprehensive review on several approaches to the rh.
- [7] Haret C Rosu. Quantum hamiltonians and prime numbers. *Modern Physics Letters A*, 18(18):1205–1213, 2003.

- [8] E Elizalde, V Moretti, and S Zerbini. On recent strategies proposed for proving the riemann hypothesis. *International Journal of Modern Physics A*, 18(12):2189–2195, 2003.
- [9] Atle Selberg. Harmonic analysis and discontinuous groups in weakly symmetric riemannian spaces with applications to dirichlet series. *Matematika*, 1(4):3–28, 1957.
- [10] Hugh L Montgomery. The pair correlation of zeros of the zeta function. In *Proc. Symp. Pure Math*, volume 24, pages 181–193, 1973.
- [11] Andrew M Odlyzko. On the distribution of spacings between zeros of the zeta function. *Mathematics of Computation*, 48(177):273–308, 1987.
- [12] Michael V Berry and Jonathan P Keating. $H = xp$ and the riemann zeros. *Supersymmetry and trace formulae: chaos and disorder*, pages 355–367, 1999.
- [13] Michael V Berry and Jonathan P Keating. The riemann zeros and eigenvalue asymptotics. *SIAM review*, 41(2):236–266, 1999.
- [14] Juan Maldacena, Stephen H Shenker, and Douglas Stanford. A bound on chaos. *Journal of High Energy Physics*, 2016(8):1–17, 2016.
- [15] Anatoly I Larkin and Yu N Ovchinnikov. Quasiclassical method in the theory of superconductivity. *Sov Phys JETP*, 28(6):1200–1205, 1969.

- [16] Koji Hashimoto, Keiju Murata, and Ryosuke Yoshii. Out-of-time-order correlators in quantum mechanics. *Journal of High Energy Physics*, 2017(10):1–31, 2017.
- [17] Fritz Haake. *Quantum signatures of chaos*. Springer, 1991.
- [18] Juan Maldacena. The large- n limit of superconformal field theories and supergravity. *International journal of theoretical physics*, 38(4):1113–1133, 1999.
- [19] Juan Maldacena, Stephen H Shenker, and Douglas Stanford. A bound on chaos. *Journal of High Energy Physics*, 2016(8):1–17, 2016.
- [20] Stephen H Shenker and Douglas Stanford. Black holes and the butterfly effect. *Journal of High Energy Physics*, 2014(3):1–25, 2014.
- [21] Stephen H Shenker and Douglas Stanford. Multiple shocks. *Journal of High Energy Physics*, 2014(12):1–20, 2014.
- [22] Stefan Leichenauer. Disrupting entanglement of black holes. *Physical Review D*, 90(4):046009, 2014.
- [23] Alexei Kitaev. Hidden correlations in the hawking radiation and thermal noise. In *Talk given at the Fundamental Physics Prize Symposium*, volume 10, 2014.
- [24] Stephen H Shenker and Douglas Stanford. Stringy effects in scrambling. *Journal of High Energy Physics*, 2015(5):1–34, 2015.

- [25] Steven Jackson, Lauren McGough, and Herman Verlinde. Conformal bootstrap, universality and gravitational scattering. *Nuclear Physics B*, 901:382–429, 2015.
- [26] Joseph Polchinski. Chaos in the black hole s-matrix. *arXiv preprint arXiv:1505.08108*, 2015.
- [27] Subir Sachdev and Jinwu Ye. Gapless spin-fluid ground state in a random quantum heisenberg magnet. *Physical review letters*, 70(21):3339, 1993.
- [28] A Kitaev. A simple model of quantum holography, talks given at the kavli institute for theoretical physics (kitp). *University of California, Santa Barbara, USA*, 7, 2015.
- [29] Alain Connes. Trace formula in noncommutative geometry and the zeros of the riemann zeta function. *Selecta Mathematica*, 5(1):29, 1999.
- [30] Michael V Berry and Jonathan P Keating. The riemann zeros and eigenvalue asymptotics. *SIAM review*, 41(2):236–266, 1999.
- [31] Simon Wozny. Self-adjoint extensions of symmetric operators.
- [32] Gieres François et al. Mathematical surprises and dirac’s formalism in quantum mechanics. 2000.
- [33] J v. Neumann. Allgemeine eigenwerttheorie hermitescher funktionaloperatoren. *Mathematische Annalen*, 102(1):49–131, 1930.

- [34] Germán Sierra. $H = xp$ with interaction and the riemann zeros. *Nuclear Physics B*, 776(3):327–364, 2007.
- [35] J Twamley and GJ Milburn. The quantum mellin transform. *New Journal of Physics*, 8(12):328, 2006.
- [36] Germán Sierra. The riemann zeros and the cyclic renormalization group. *Journal of Statistical Mechanics: Theory and Experiment*, 2005(12):P12006, 2005.
- [37] Masanori Hanada and So Matsuura. *MCMC from Scratch: A Practical Introduction to Markov Chain Monte Carlo*. Springer Nature, 2022.
- [38] Masanori Hanada. Markov chain monte carlo for dummies. *arXiv preprint arXiv:1808.08490*, 2018.